



Journal of Physical Sciences
BIBECHANA

Editor-in-Chief

Devendra Adhikari

Professor, Physics
MMAMC, T.U.

Published by
Department of Physics
Mahendra Morang Adrash Multiple Campus
T.U., Biratnagar

BIBECHANA

ISSN 2091-0762 (Print), 2382-5340 (Online)

Journal homepage: <http://nepjol.info/index.php/BIBECHANA>

Publisher: Department of Physics, Mahendra Morang A.M. Campus, TU, Biratnagar, Nepal

Study of dust color temperature and visual extinction distribution of a far infrared cavity at 60 and 100 μm IRAS map around the AGB star at galactic latitude 8.6°

A. K. Gautam*, B. Aryal**

Central Department of Physics, T.U., Kirtipur, Nepal

Email: arjungautamnpi@gmail.com*, **baryal@tucdp.edu.np

Article Information

Received: July 02, 2019

Accepted: September 14, 2019

Keywords:

Far infrared cavity

Far infrared loops

AGB stars

Dust color temperature

Dust mass

ABSTRACT

The dust-grain structure in the far infrared region under IRAS (Infrared Astronomical Satellite) Survey was studied using sky view virtual observatory. In order to find the possible far infrared cavity, we used SIMBAD database. In this paper, we discuss about the dusty environment of a far infrared cavity around the AGB star located at R.A. (J2000) = $01^{\text{h}} 41^{\text{m}} 01^{\text{s}}$ and Dec (J2000) = $71^\circ 04' 00''$ lying within far infrared loop G125+09 in the far infrared IRAS maps. A cavity like structure (major diameter ~ 2.55 pc & minor diameter ~ 0.77 pc) is found to lie at R.A. (J2000) = $01^{\text{h}} 46^{\text{m}} 57.2^{\text{s}}$ and DEC (J2000) = $71^\circ 24' 57.1''$, located at a distance ~ 220 pc from the star. We studied the distribution of flux density, dust color temperature, dust mass, inclination angle, visual extinction and FIR spectral distribution of the cavity. We further studied the distribution of Planck function along extension and compression. The dust color temperature is found to lie in the range (19.7 ± 0.65) K to (21.1 ± 0.35) K which shows the cavity is isolated and stable. Product of visual extinction and dust color temperature is found to be less than one. A possible explanation of the results will be discussed.

DOI: <https://doi.org/10.3126/bibechana.v17i0.25839>

This work is licensed under the Creative Commons CC BY-NC License. <https://creativecommons.org/licenses/by-nc/4.0/>

1. Introduction

There are three types of stars according to their mass. They are low mass stars, intermediate mass stars and massive stars. Their proportion in existence is 1: 10: 1000. Most of the stars spend their half-life in main sequence. When fusion of hydrogen is exhausted in the main sequence, the star leaves the main sequence and rises up towards right side. This stage of evolution is called red giant branch (RGB)

phase. During this phase, the star expands but core contracts as a result luminosity increases. As the luminosity reaches nearly $10^3 L_\odot$, inert He core burns means He shell flash takes place and the star moves horizontally with almost constant luminosity. This stage of stellar evolution is called horizontal branch (HB). After around 10^8 years, He core exhausts. At this condition, He core leaves its space and two burning shells i.e. H-burning shell and He-

burning shell are produced leaving C/O core as a result the star moves up parallel to RGB which is called asymptotic giant branch (AGB) Herwig [1].

For low mass stars having masses $< 0.8M_{\odot}$, there is not sufficient temperature for fusion of hydrogen so that they can't change in to Asymptotic giant branch (AGB) stars. Actually low and intermediate mass stars in the range ($0.8M_{\odot} < M < 8.0M_{\odot}$) are the AGB stars which is the final nuclear burning stage. This phase of evolution is characterized by two nuclear burning shell of hydrogen and helium where hydrogen burning shell lies below the convective envelope and helium burning shell lies above the electron-degenerate core of carbon and oxygen, or for the most massive AGB stars a core of oxygen, neon, and magnesium [1]. This AGB stage is characterized by low surface effective temperatures (below 3500K) and intense mass loss (from 10^{-7} to $10^{-4} M_{\odot}\text{yr}^{-1}$) [2].

Interstellar medium consists of matter and field. Matter contains gas and dust. First evidence of dust in the ISM was first justified by interstellar extinction curve. Dusty circumstellar envelopes will form at the distance of several stellar radii. Dust grains in the envelopes absorb stellar radiation say uv radiation and re-emit infrared radiation so AGB stars are important infrared sources. The mass loss process plays an important role in the evolution of AGB stars. Statistics of a large sample of AGB stars would help to constrain the evolution of dust envelope. There are mainly three types of AGB stars: the O-rich with $C/O < 1$ and mainly silicate-type grains in the outflow, C-rich with $C/O > 1$ and mainly carbonaceous grains in the envelopes and S-type with $C/O \sim 1$. Due to different dust compositions of these AGB stars, different infrared spectral features are obtained which can be used to distinguish the groups of the stellar objects .

He-core burning phase is about 10 times shorter than the H-core burning shell so that the He-core burning leaves a C/O core behind that is surrounded by both a hydrogen and helium burning shell. For low and intermediate mass stars, carbon doesn't ignite and C/O core contracts and becomes electron degenerate.

During the early AGB phase, the abundance of He in the center goes to zero where He-burning continues in a shell around a degenerate C-O core. In the meantime, the H- layer around the helium shell expands and cools sufficiently so that hydrogen burning shell is extinguished. Convective envelope sets in and moves inwards and second dredge-up takes place. He shell is the main source for nuclear production so that it burns outward and reaches the hydrogen shell. In case of thermally pulsating AGB phase, helium shell becomes thin and remains thermally unstable as a result thermal pulses are produced. In each thermal pulse, luminosity of helium shell nearly approaches $10^8 L_{\odot}$ [3]. The production of such high luminosity in helium shell is called He shell flash or thermal pulse which is used to expand the outer layers. Such strong expansion drives the H shell cooler and less dense as a result H shell is extinguished. The inner edge of deep convective envelope can then move inward and mix to the surface products of internal nucleosynthesis. This mixing process which occurs periodically after each TP is known as third dredge-up which is the mechanism for producing carbon stars. During TP-AGB phase, main dominant source of nuclear energy is the hydrogen shell. Thermally pulsating AGB phase is the phase after the first thermal pulse to the time when the star ejects its envelope.

In this paper, we study the physical properties of far infrared cavity, that we investigated during a systematic search on IRAS maps, located close to a carbon-rich AGB star named AGB01+71 at 8.6° Galactic latitude. In section 2, we describe methods of calculation. A brief description of the result and discussion will be given in the section 3. Finally, we conclude our results in the section 4.

2. Methods

We found a far infrared cavity at 60 and 100 micron IRAS maps around an Asymptotic Giant Branch star named AGB 01+71. We briefly describe a method for calculation of dust color temperature, dust mass and visual extinction of the far infrared cavity around the AGB star. Additionally far infrared spectral distribution of the cavity is also described.

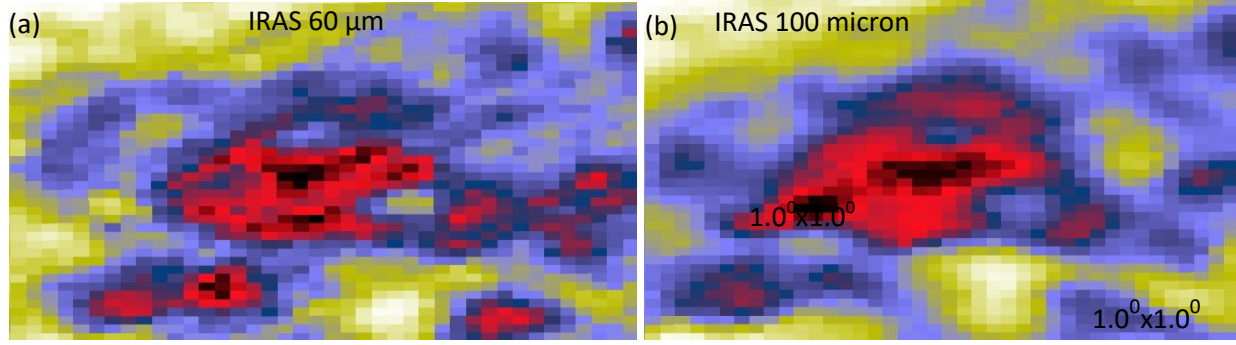


Fig. 1: (a) and (b) are the JPEG images of the far infrared cavity at 60 μm and 100 μm IRAS maps around the AGB 01+71 centered at R.A. (J2000) = $01^{\text{h}}46^{\text{m}}57.2^{\text{s}}$, Dec. (J2000) = $71^{\circ}24'57.1''$, located within far infrared loop G125+09.

Dust color temperature

For the calculation of dust color temperature, we adopt the method proposed by Schnee et al. [4] and Dupac et al. [5]. According to Schnee et al. [4], dust color temperature of the emission at a wavelength λ_i is given by

$$T_d = \frac{-96}{\ln\{R+(0.6)^{(3+\beta)}\}} \quad (1)$$

$$\text{where, } R = \frac{F(60 \mu\text{m})}{F(100 \mu\text{m})}$$

$F(60 \mu\text{m})$ and $F(100 \mu\text{m})$ are the flux densities in 60 μm and 100 μm respectively and Eq. (1) is used for calculation of the dust color temperature. The spectral emissivity index (β) depends on dust grain properties like composition, size, and compactness. For a pure blackbody would have $\beta = 0$, the amorphous layer-lattice matter has $\beta \sim 1$, and the metals and crystalline dielectrics have $\beta \sim 2$ which is used in our calculations.

Planck function

The value of Planck's function depends on the wavelength (frequency), and hence the temperature. Finally it is used to calculate dust mass. In 1900, Planck proposed a relation which is named as Planck's function. According to him, the Planck's function is given by

$$B(\nu, T) = \frac{2h\nu^3}{c^2} \left[\frac{1}{e^{\left(\frac{h\nu}{kT}\right)} - 1} \right] \quad (2)$$

where, h = Planck's constant, c = velocity of light, ν = frequency at which the emission is observed, λ = wavelength of the radiation and T = temperature of each pixel.

Dust mass

For the calculation of dust mass, first we need the value of flux density ($F\nu$) at 100 μm maps and we use the expression given by [6],

$$M_d = \frac{4a\rho}{3Q(\nu)} \frac{F(\nu)D^2}{B(\nu, T)} \quad (3)$$

where, weighted grain size (a) = 0.1 μm , grain density (ρ) = 3000 kg m^{-3} , grain emissivity (Q_ν) = 0.0010 (for 100 μm) [7]. So the equation (3) reduces to

$$M_{\text{dust}} = 0.4 \left[\frac{S_\nu D^2}{B(\nu, T)} \right] \quad (4)$$

We use equation (4) to calculate dust mass of the cavity.

Inclination angle

The inclination angle (i) is the angle between the line-of-sight and the normal vector of the plane of the loops. Here, the long axis of KK-loops can be assumed to be inclined by a certain angle with respect to the plane of the sky. In such case, the inclination angle can be estimated using Holmberg [8] formula:

$$\cos^2 i = \frac{b^2}{a^2 - q^2} \quad (5)$$

where b/a is the axial ratio measured and q is the intrinsic flatness of the cavity. As suggested by Holmberg [8] for oblate spheroid structure, we used the value of intrinsic flatness $q = 0.33$.

Estimation of visual extinction

For estimation of visual extinction, Wood et al. [9] has provided an empirical formula using optical depth at $100 \mu\text{m}$. According to them, we have

$$A_v(\text{mag}) = 15.078 \left(1 - e^{-\frac{\tau_{100}}{641.3}} \right) \quad (6)$$

where

$$\tau_{100} = \frac{F_\lambda(100\mu\text{m})}{B_\lambda(100\mu\text{m}, T_d)} \quad (7)$$

is optical depth at $100 \mu\text{m}$ wavelength. Here F_λ is flux density and B_λ is Planck function at $100 \mu\text{m}$ wavelength.

3. Result and Discussion

Structure: Contour maps

Using sky view virtual observatory and its JPEG and FITS images in the far infrared region, we found an isolated far infrared cavity in the $100 \mu\text{m}$ and $60 \mu\text{m}$ IRAS maps at R.A. (J2000) = $01^{\text{h}} 46^{\text{m}} 57.2^{\text{s}}$, Dec. (J2000) = $71^{\circ} 24' 57.1''$, located within far infrared loop G125+09. We used Aladin2.5 software in FITS image of sky view virtual observatory of the cavity and have studied size, dust color temperature, dust mass, inclination angle, visual extinction and spectral distribution of the FIR cavity. We selected contour level 1-85 in such a way that it circles the cavity. JPEG images of the cavity at $60 \mu\text{m}$ and $100 \mu\text{m}$ IRAS map are shown in the fig.1 (a) and (b) respectively.

Distribution of flux density

Flux densities at $60\mu\text{m}$ and $100\mu\text{m}$ have been measured by using ALADIN 2.5 software. Distribution of flux density within the core region of the cavity has been studied. We have plotted a graph between $F(100)$ and $F(60)$ with the help of ORIGIN 5.0 which is shown in figure 2(a) to calculate average dust color temperature. From the linear fit, slope of the line was 0.17, correlation coefficient (R) = 0.68. The linear equation of the

fitted line is, $y = -1.01+0.17x$. Using the slope of best fitted plot, average dust color temperature has been found as 22.2 K which is used to calculate error in calculated dust color temperature.

Again distribution of flux density at $100 \mu\text{m}$ flux density within the contour level with right ascension (R.A.) and declination (Dec.) are plotted in contour map by using ORIGIN 8.0 and is shown in figure 2(b). Graph shows that all the fluxes from minimum to maximum lie within the contour level. Most of the maximum flux regions lie at the boundary.

Dust color temperature and its variation

Schnee et al.[4] has derived an expression for calculation of dust color temperature. Gautam and

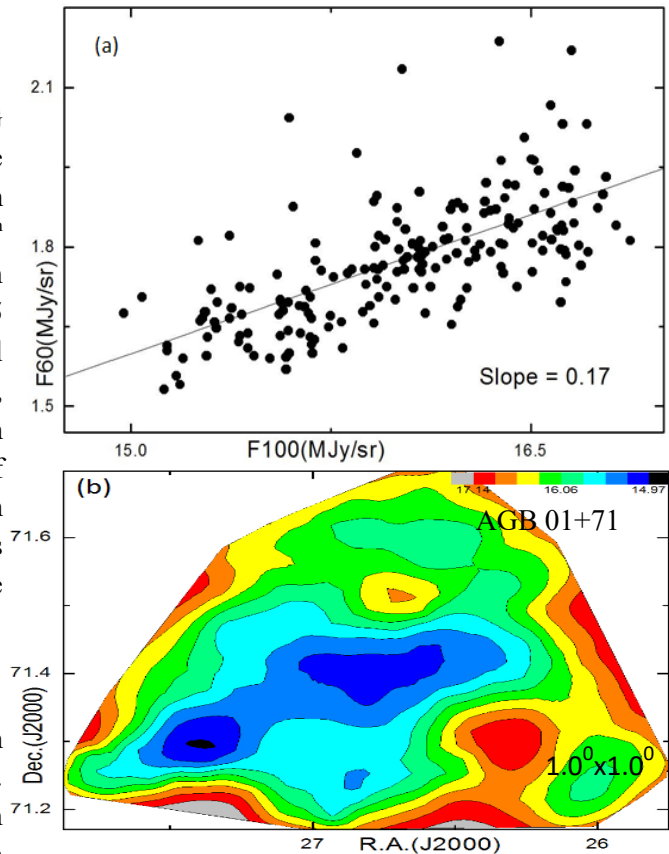


Fig.2: (a) The $100\mu\text{m}$ versus $60\mu\text{m}$ flux density in the region of interest and (b) Contour map at $100\mu\text{m}$ flux density where the AGB star is located at the center R.A. = $01^{\text{h}} 46^{\text{m}} 57.2^{\text{s}}$, Dec. (J2000) = $71^{\circ} 24' 57.1''$.

Aryal [10] used the formula for calculation of dust color temperature. We also adopted similar method for calculation of dust color temperature in the core region of our interest. For the calculation of temperature we choose the value of $\beta = 2$ following the explanation given by Dupac et al. [5]. Variation of temperature with corresponding R.A.(J2000) and Dec.(J2000) are plotted by using ORIGIN 8.0 and the graph is shown in figure 3(a). Graph shows that temperature distributions are in separate cluster but minimum temperature region is little bit shifted from minimum flux density which is unusual behavior. Such type of nature is obtained due to external factors.

The region in which minimum and maximum temperature is found in the range (19.7 ± 1.25) K to (21.1 ± 0.55) K with low offset temperature. Such low offset temperature variation shows that there is

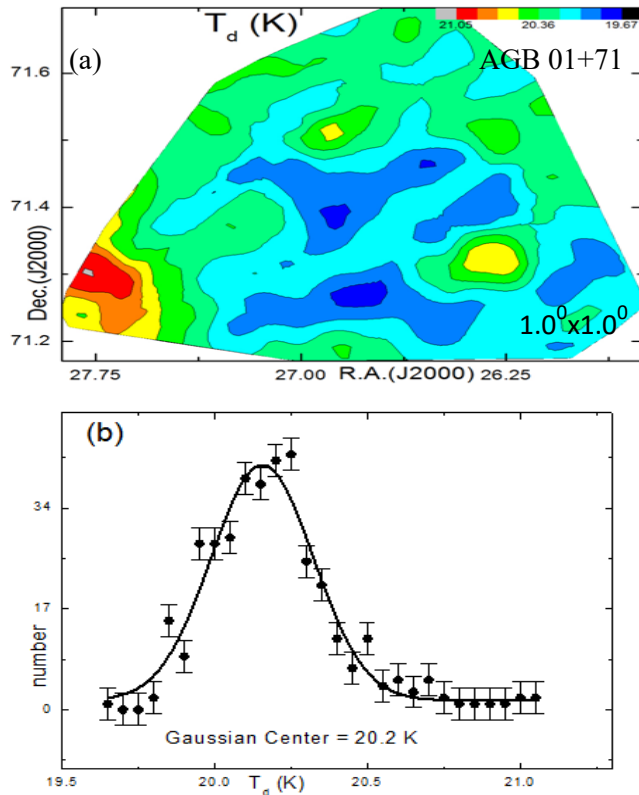


Fig. 3: (a) Contour map of dust color temperature and (b) Gaussian fit of dust color temperature. The far infrared cavity is centered at R.A. = $01^{\text{h}} 46^{\text{m}} 57.2^{\text{s}}$, Dec. (J2000) = $71^{\circ} 24' 57.1''$.

symmetric outflow or symmetric distribution of density and temperature. It further suggests that particles are independently vibrating. Gaussian fit of dust color temperature is Gaussian like with positive skewness shown in figure 3(b). When this result is compared with the result obtained in Jha et al. [11] where temperature variation is 19.4 K to 25.3 K so our result is also comparable with that result. In the contour map, minimum flux and minimum temperature region are shifted which is due to some external factors possibly due to AGB wind.

Size of the structure

Major and minor diameter of the structure can be easily calculated by using a simple expression i.e., $L = R \times \theta$, where $R = 220$ pc is the distance of the structure and $\theta = \text{pixel size (in radian)}$. After calculation the major and minor diameter of the cavity are found to be 2.55 pc and 0.77 pc respectively. Thus, the size of the structure is $2.55 \text{ pc} \times 0.77 \text{ pc}$.

Dust mass estimation and its variation

For the calculation of dust mass, we need the distance of the structure (cavity) from earth. The distance of the structure is 220 pc [3]. After calculation of dust color temperature and Planck function, we have calculated mass of the cavity. Average mass of each pixel has found to be 4.91×10^{25} kg and total mass of the structure is 1.86×10^{28} kg i.e $0.0094 M_{\odot}$. But mass of dust obtained around white dwarf WD 1003-44 in Aryal et al. [12] is $0.08 M_{\odot}$. It means mass of dust around AGB Star is less than White Dwarf.

Distribution of dust mass in the contour map is shown in figure 4(a) which shows that minimum temperature region is denser and lie at the maximum mass region in the selected contour which is usual trend means distribution of mass follows cosmological principle. It means distribution of dust mass follow cosmological principle i.e their distribution is homogeneous and isotropy. Figure 4(b) is the Gaussian fit where the

data more or less follow Gaussian distribution with negative skewness.

Distribution of Planck function with diameters

Figure 5(a) and (b) show the distribution of Planck function along major and minor diameters where the dust particles are oscillating non-uniformly with very low correlation coefficient (R). There is no systematic trend of their distribution in both cases so that the dust particles about the diameters are not in thermal equilibrium means they are oscillating in order to get dynamical equilibrium [10].

Variation of visual extinction

Figure 6 (a) is contour map of visual extinction and 6(b) is a linear fit of the scattered plot between visual extinction and dust color temperature. From figure 3(a) and 6(a), it is found that higher the temperature, lower the visual extinction and vice-versa. The figure 6(b) shows a systematic trend with high correlation coefficient i.e., -0.92, which shows that there is best correlation between the data. From the linear fit, we found a relation between visual extinction and dust color temperature. The relation is $(A_V \times T_d) < 1$ which also supports our result.

FIR Spectral Distribution

A graph between wavelength and flux density is called spectral distribution. We studied spectral distribution of the far infrared cavity around the AGB star named AGB01+71 where we found positive slope in transition from 12 μm to 25 μm and 60 μm to 100 μm but there is negative slope in transition from 25 μm to 60 μm which is one finding of this work shown in figure 7.

4. Conclusion

The physical properties of the far infrared cavity around the AGB01+71 star located within far infrared loop G125+09 are measured and analyzed. From the calculated value, distribution of flux density, dust color temperature, Planck function, dust mass and visual extinction of the cavity were studied. Following are the conclusions:

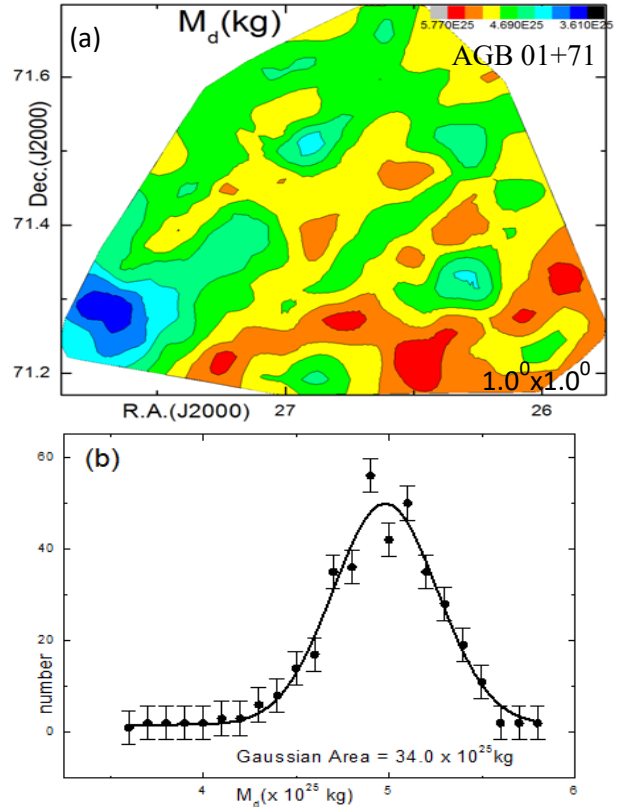


Fig.4: (a) Contour map of dust mass and (b) Gaussian fit of dust mass. The far infrared cavity is centered at R.A. = $01^{\text{h}} 46^{\text{m}} 57.2^{\text{s}}$, Dec. (J2000) = $71^{\circ} 24' 57.1''$.

- The major and minor diameter of the far infrared cavity was found to be 2.55 pc and 0.77 pc respectively.
- The maximum temperature (21.1 ± 0.25) K was found at R.A.(J2000) = 27.820 & Dec.(J2000) = 71.310 27.80 and minimum temperature (19.7 ± 0.65) K was found at R.A.(J2000) = 26.780 & Dec.(J2000) = 71.26026.80, with low offset temperature which suggests that the cavity is isolated and stable.
- Inclination angle is found to be 910 i.e., edge-on.
- In general, minimum flux and minimum temperature lie at same point in the pixel but in this case minimum temperature is shifted which may be due to external factors, possibly wind emitted from the AGB star. Similarly maximum temperature region is the densest region which is normal behavior. It means distribution of dust mass follow cosmological

- principle.
- Total mass of the cavity was found to be 1.86×10^{28} Kg and that of average mass was 4.91×10^{25} kg.
- Linear fit of scattered plot between visual extinction and dust color temperature shows that there is a systematic trend and visual extinction decreases with increase in dust color temperature and vice-versa.
- Distribution of Planck function along extension and compression is non-uniform so that dust particles are not in thermal equilibrium along the diameters.

- FIR spectral distributions of the cavity showed similar nature in transition from $12 \mu\text{m}$ to $25 \mu\text{m}$ and $60 \mu\text{m}$ to $100 \mu\text{m}$. Negative slope in transition from $25 \mu\text{m}$ to $60 \mu\text{m}$ is our finding regarding FIR spectral distribution in cavities. This suggests that the number density of dust particles are found to be less (than expected) in $60 \mu\text{m}$ region.

We intend to study the role of carbon-rich AGB star to form the far-infrared cavity in the future.

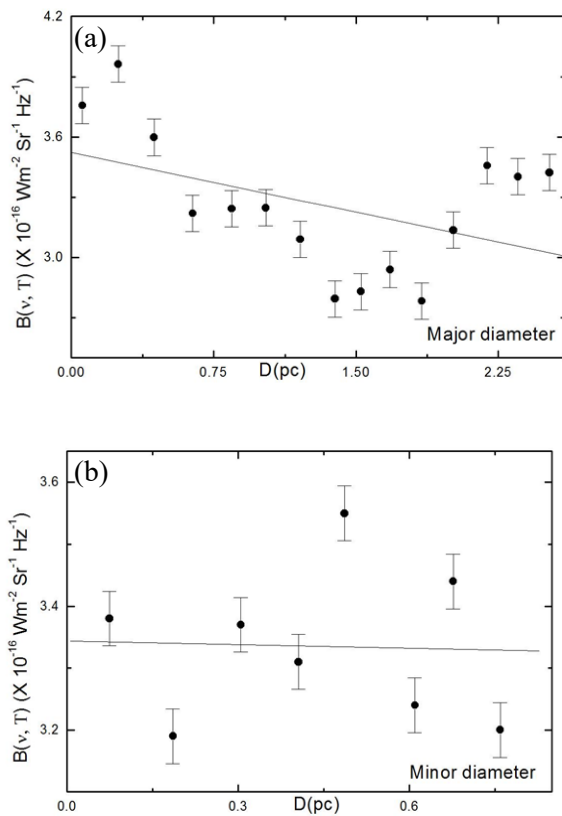


Fig.(5):(a) Linear fit of scattered plot between major diameter and Planck function and (b) Linear fit of scattered plot between minor diameter and Planck function of the cavity centered at R.A. = $01^{\text{h}} 46^{\text{m}} 57.2^{\text{s}}$, Dec. (J2000) = $71^{\circ} 24' 57.1''$.

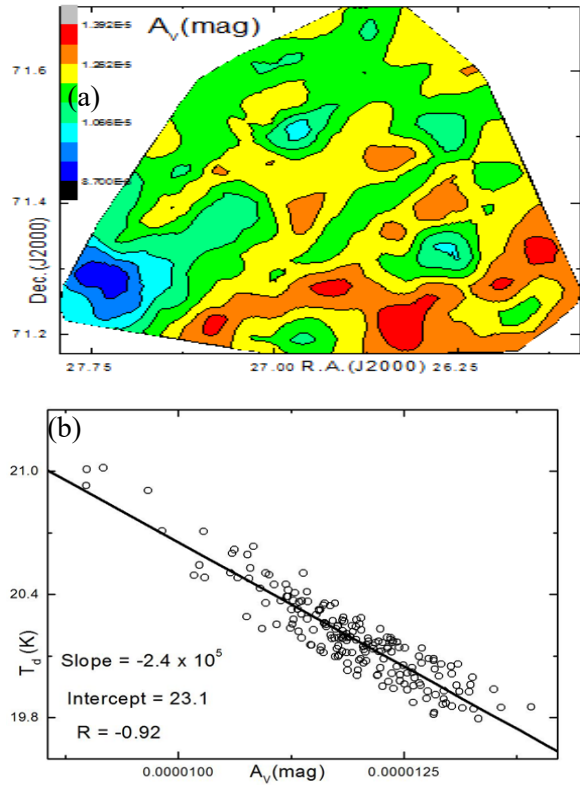


Fig. 6: (a) Contour map of visual extinction and (b) a linear fit of the scattered plot between visual extinction and dust color temperature of the far infrared cavity centered at R.A. = $01^{\text{h}} 46^{\text{m}} 57.2^{\text{s}}$, Dec. (J2000) = $71^{\circ} 24' 57.1''$.

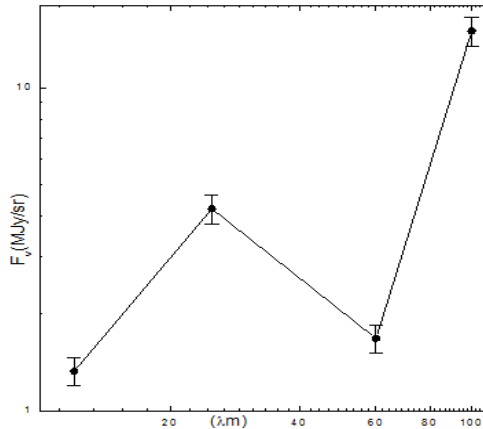


Fig. 7: Far infrared spectral distributions of the cavity located nearby AGB star AGB01+71.

Acknowledgements

We are grateful to the Department of Astro-Particle Physics, Innsbruck University, specially to Prof. R. Weinberger for invoking us to work on dusty environments around AGB stars. This research has made use of Sky View Virtual Observatory, Aladin v2.5 and NASA/IPAC Extragalactic Database (NED).

References

- [1] F. Herwig, Evolution of Asymptotic Giant Branch Stars, *Annu. Rev. Astron. Astrophys* 43 (2005) 435-479.
<https://doi.org/10.1146/annurev.astro.43.072103.150600>
- [2] L. Seiss, M. L. Pumo, Evolutionary Properties of Massive AGB Stars, *Memorie della Societa Astronomica Italiana* 77 (2006) 822-827.
- [3] A. L. Karakas, J. C. Lattanzio, O. R. Pols, Parameterising the third dredge-up in asymptotic giant branch stars, *Astron. Soc. Aust.* 19 (2002) 515-38.
<https://doi.org/10.1071/AS02013>
- [4] S.L. Schnee, N.A. Ridge, A. A. Goodman, G. L. Jason, A Complete Look at the Use of IRAS Emission Maps to Estimate Extinction and Dust Temperature, *The Astrophysical Journal* 634 (2005) 442-450.
<https://doi.org/10.1086/491729>
- [5] X. Dupac, J. P. Bernard, N. Boudet, M. Giard, J. M. Lamarre, C. Meny, F. Pajot, I. Ristorcelli, G. Serra, Stepnik, J. P. Torre, Inverse Temperature Dependence of the Dust Submillimeter Spectral Index, *Astronomy & Astrophysics* 404 (2003) L11-L15.
<https://doi.org/10.1051/0004-6361:20030575>
- [6] R. H. Hildebrand, The determination of cloud mass and dust characteristics from sub millimeter thermal emission, *Royal Astronomical Society*, 24 (1983) 267-282.
- [7] K. Young, T. G. Phillips, G. R. Knapp, Circumstellar Shells Resolved in IRAS Survey Data II Analysis, *Astrophysical Journal* 409 (1993) 725-738.
<https://doi.org/10.1086/172702>
- [8] Erik Holmberg, Investigations of the systematic errors in the apparent diameters of the nebulae, *MeLus*, 117 (1946) 3H.
- [9] D. O. S. Wood, P. C. Myers, D. A. Daugherty, IRAS images of nearby dark clouds, *The Astrophysical Journal Supplement* 95 (1994) 457-501.
<https://doi.org/10.1086/192107>
- [10] A. K. Gautam, B. Aryal, A study of four low-latitude ($|\ell| < 100$) far-infrared cavities, *Journal of Astrophysics and Astronomy* 40 (2019)16. 10.1007/s12036-019-9578-1.
<https://doi.org/10.1007/s12036-019-9578-1>
- [11] A. K Jha, B. Aryal, R. Weinberger A study of dust color temperature and dust mass distributions of four far infrared loops, *North America Astronomical Society, Mexico* 53 (2017) 467-476.
- [12] B. Aryal, and R. Weinberger, Dust structure around White Dwarf WD 1003-44 in 60 and 100 μm Iras Survey, *The Himalayan Physics II* (2011) 5-10.
<https://doi.org/10.3126/hj.v2i2.5202>